Visualization of heated coaxial jet flow and its noise radiation

Video

Author(s):
Gloor, Michael; Kleiser, Leonhard; Favre, Jean

Publication date:
2014

Permanent link:
https://doi.org/10.3929/ethz-a-010151253

Rights / license:

VISUALIZATION OF HEATED COAXIAL JET FLOW AND ITS NOISE RADIATION

Michael Gloor and Leonhard Kleiser[*]

Institute of Fluid Dynamics, ETH Zurich, 8092 Zurich, Switzerland

Jean M. Favre

CSCS, Swiss National Supercomputing Centre, 6900 Lugano, Switzerland

Abstract

This document serves as a brief explanation to the movie *"Large Eddy Simulation of Heated Coaxial Jet Flow and its Noise Radiation"* [Gloor et al., 2014]. The visualizations are based on the numerical simulation *LES1a*, which is fully documented in Gloor [2014].

1 Flow and simulation parameters

The flow development of a heated coaxial jet is modeled by the filtered Navier-Stokes equations, which are solved numerically in non-dimensional form (Large Eddy Simulation approach). Length scales are non-dimensionalized by the radius of the core jet R_1^*, where the superscript $*$ indicates a dimensional quantity. Velocities are scaled with the axial centerline velocity at the inlet w_0^* and the density ρ^*, temperature T^* and viscosity μ^* are scaled with their reference values at $r = z = 0$. The non-dimensional time is given by $t = t^* w_0^* / R_1^*$. The pressure p^* is non-dimensionalized by the dynamic pressure $\rho_0^* w_0^{*2}$. The Reynolds and Mach numbers are defined as

$$Re_0 = \frac{\rho_0^* w_0^* R_1^*}{\mu_0^*}, \quad Ma_{p,0} = \frac{w_0^*}{a_0^*}, \quad Ma_{p,\infty} = \frac{w_0^*}{a_\infty^*}, \tag{1}$$

where a_0 is the speed of sound based on jet-centerline conditions and a_∞ is the speed of sound in the ambient fluid. The subscripts $(\cdot)_p$ and $(\cdot)_s$ refer to the primary core and the secondary stream, respectively. Simulation parameters are listed in Tab. 1, whereas the grid parameters are given in Tab. 2.

Table 1: Simulation parameters. $T_s/T_\infty = 1$.

ID	$Ma_{p,0}$	$Ma_{p,\infty}$	$Ma_{s,\infty}$	Re_0	w_s/w_p	T_p/T_s
LES1a	0.88	1.44	0.917	250000	0.637	2.7

---

[*]Electronic address: `michael.reto.gloor@alumni.ethz.ch`; Corresponding author

Table 2: Employed numerical grid for simulation listed in Tab. 1.

N_θ	N_z	N_r	Δr_{min}	Δz_{min}
128	1600	1024	0.0221	0.0654

2 Visualization

This section briefly discusses the individual sequences of the movie [Gloor et al., 2014]. A detailed discussion of the underlying physics is given in Gloor [2014].

2.1 Temperature distribution

The first sequence of the movie shows the instantaneous temperature distribution of the heated coaxial jet on a two-dimensional slice, see Fig. 1. It shows the mixing between hot (red) and cold (blue) fluid. Only the primary stream of the coaxial jet is heated $(T_p/T_s = 2.7)$ whereas the secondary stream has the same temperature as the ambient fluid $(T_s/T_\infty = 1)$. For better visibility during the following sequences, the ambient temperature is only shown in the vicinity of the interface between the hot and the cold fluid.
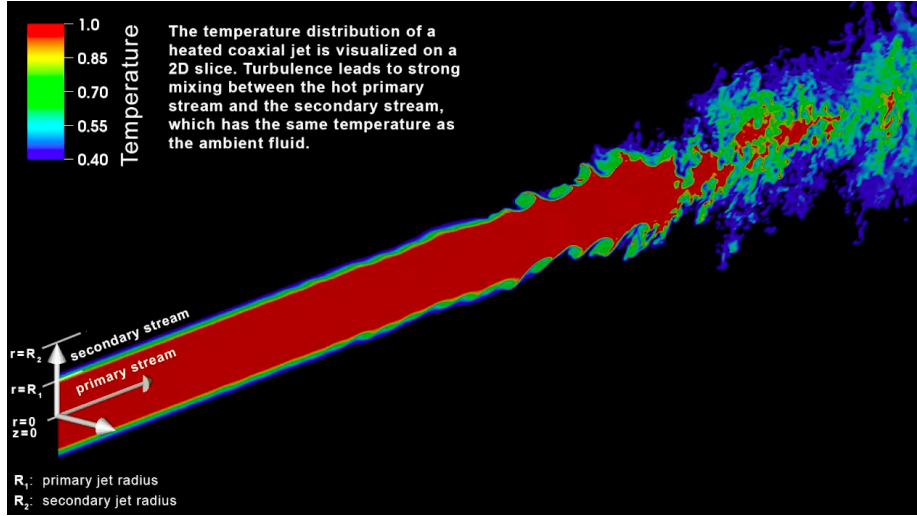

Figure 1: Temperature distribution.

2.2 Inner shear-layer instabilities

The second sequence (Fig. 2) visualizes the Kelvin-Helmholtz instabilities that develop in the inner shear layer along $r = R_1$. The vortices are visualized by the λ_2 vortex-identification criterion [Jeong and Hussain, 1995]. The visualization technique is based on a volume-rendering method [VisIt]. In addition to the specification of a color scheme, this method allows the definition of transparency levels for the specific color range. These transparency levels are indicated on top of the λ_2 colorbar. Using this technique, multiple smooth surfaces can be selected for visualization.
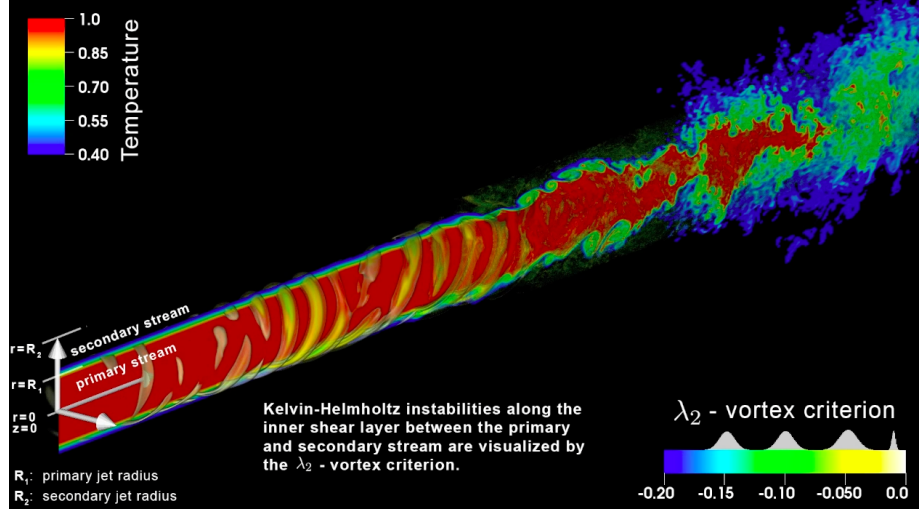

Figure 2: Temperature distribution and inner shear-layer instabilities.

2.3 Inner and outer shear-layer instabilities

In addition to the instabilities along the interface between the primary and secondary stream, Fig. 3 also shows the Kelvin-Helmholtz instabilities that develop along the velocity shear layer between the secondary stream and the ambient flow. These instabilities lead to the laminar-turbulent transition.
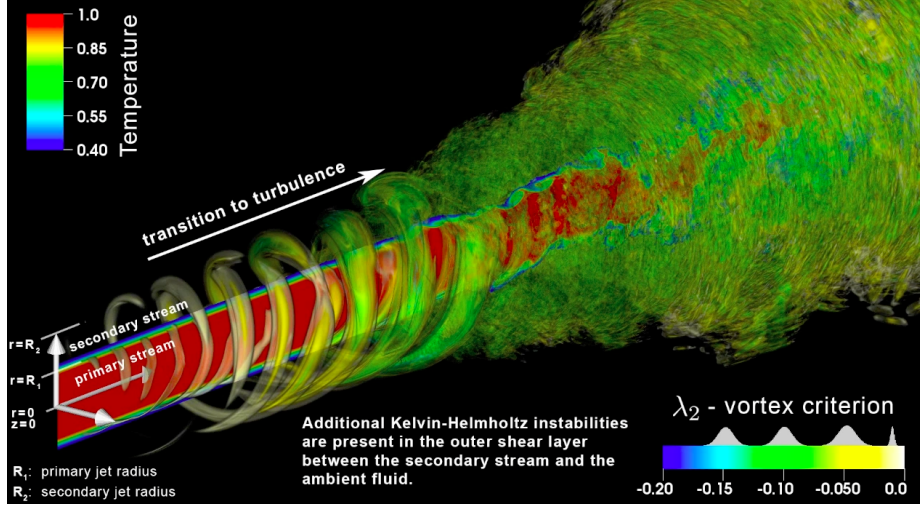
Figure 3: Temperature distribution, inner and outer shear-layer instabilities.

2.4 Streamwise transition

A three-dimensional visualization of the laminar-turbulent transition is shown in Fig. 4 using the λ_2 vortex-identification criterion. The dominance of the (forced) helical instabilities ($n = 3$) in the upstream region can be well observed from this visualization. Cross-stream slices of instantaneous axial velocity, temperature and vorticity magnitude are also visualized.
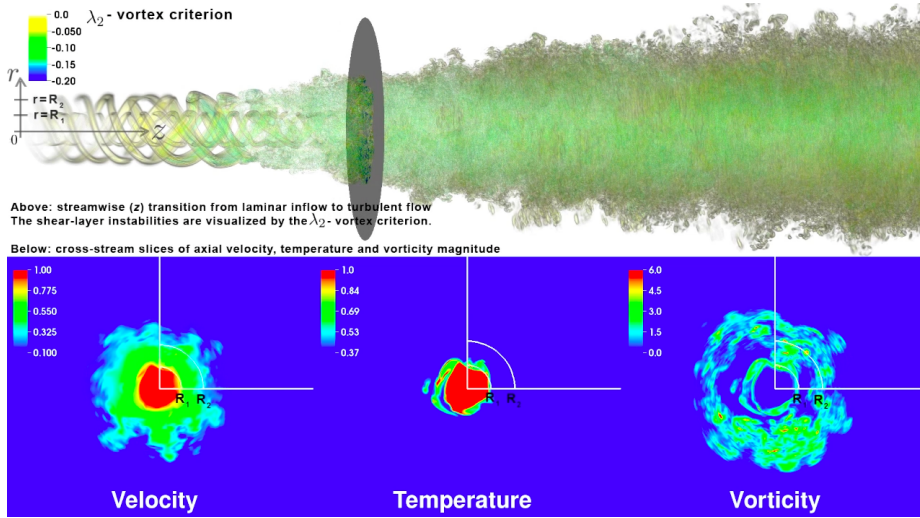

Figure 4: Top: λ_2 vortex-identification criterion; below: (r, θ) slices of axial velocity w (left), temperature T (middle) and vorticity magnitude $|\omega|$ (right)

2.5 Noise radiation

Figure 5 visualizes the three-dimensional structure of hydrodynamic instability waves, which are limited to the jet near field, and acoustic waves that radiate into the ambient flow. The visualization shows that pressure waves are emitted from the unsteady jet flow and propagate towards the acoustic far field with dominant radiation at approximately $30° \lesssim \phi \lesssim 45°$ with respect to the jet axis. Additionally, the pressure fluctuations $p' = p - \langle p \rangle$ are visualized on a horizontal plane.
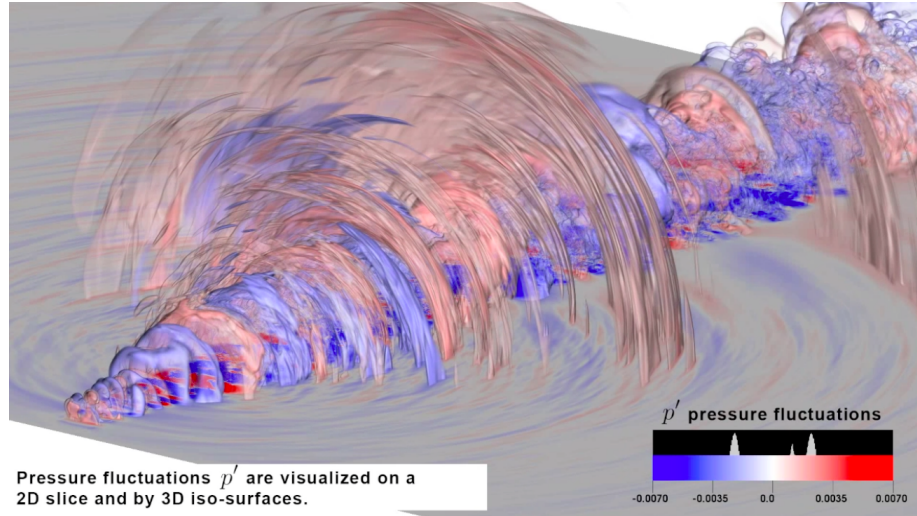

Figure 5: Pressure fluctuations.

Acknowledgments

References

Michael Gloor. *Numerical investigation on hydrodynamic stability and noise radiation of coaxial jet flows*. PhD thesis, ETH Zurich, 2014.

Michael Gloor, Leonhard Kleiser, and Jean M. Favre. Visualization of heated coaxial jet flow and its noise radiation. Available online at http://e-collection.library.ethz.ch, May 2014.

Jinhee Jeong and Fazle Hussain. On the identification of a vortex. *J. Fluid Mech.*, 285:69–94, 1995.

VisIt. Available online at https://wci.llnl.gov/codes/visit/.